DOI: 10.13009/EUCASS2019-368

The effect of single defect of RDX crystal on shock sensitivity of RDX/Al mixtures by ReaxFF-MD simulations

Ning Wang[1,2], Jun Li[1,2], Lu Wang[3], Liguo Cheng[1,2], Jing Su[1,2], Xu Xiao[2] and Jiefan Zhang[2]

1.Science and Technology on Aerospace Chemical Power Laboratory, Xiangyang 441003, China

2.Aerospace Industry Research Center of Solid Propellant Safety Technology, Xiangyang 441003, China

3.Hubei Institute of Aerospace Chemotechnology, Xiangyang 441003, China

sdwn8211@163.com, aqzx9084@163.com, wl18671016755@163.com, clgcasc42@163.com, sujing42s@163.com, xiaoxu56@126.com, zhangjf_92619@163.com

Abstract

We used ReaxFF molecular dynamics simulations to study single defect of RDX on shock sensitivity of RDX/Al. The results show that internal defects play a key role in disordering crystal arrangement and in enhancing decomposition rate at initial impact stage. RDX/Al with surface defect concentrate on defect position to cause structure damage and local chemical reactions to generate more NO_2, not interfacial reaction between RDX and Al. HMX inclusions exhibit difference, which depend on the location whether on RDX surface or enclosed by RDX crystals. Such basic information is necessary for improving crystal quality of energetic materials in LOVA propellants.

1. Introduction

The characteristics of the explosive ingredients used as high energy propellant and polymer bonded explosive (PBX), play an important role in determining the risk of an unintentional explosive response to external threats, like a fire, bullet or fragment impact, sympathetic detonation, and shock initiation. The relationship between crystal properties and shock sensitivity has been an active research topic for more than two decades. The crystal properties of energetic crystals[1, 2] mainly include grain size and distribution, crystal internal defect, crystal surface shape and roughness, and a range of cyclotetramethylene tetranitramine (HMX) content. Particularly, experimental studies have shown that crystal properties have strong effects on the shock sensitivity of high explosives.[3-6]

Many researchers believe that the reduction of internal void amounts can significantly reduce the shock sensitivity. Stoltz[5] investigated the influence of internal void size ranging from 10 Å to 20 mm in cyclotrimethylene trinitramine (RDX) crystal on the shock sensitivity of PBX, indicating that the critical shock initiation pressure decreases from 5.17 GPa to 2.39 GPa with increasing void size. Hua[6] found that the shock sensitivity of PBX increases with increasing defect size and amount of RDX and HMX crystals. Some of these internal voids, which are usually solvent inclusions resulting from crystallization processes, can also have large effects on the shock sensitivity of high explosives.[4]

However, Czerski[7] found that the internal void count does not correlate with the sensitivity of a granular bed and that crystals with defects can be insensitive in this case. Sensitivity in their tests was correlated with the presence of surface "dimples" for particles which were 10-30 μm in size, For large particles (100-300μm in size), more angular crystals were more sensitive. Bellitto[8] stated that a statistically significant relationship exists between surface roughness characteristics and shock sensitivity and that it is not the average roughness of the material but its consistency across the crystal surface that plays the key role in influencing the sensitivity.

As part of a Round Robin program, the product quality of seven commercial RDX grades was compared with its shock initiation at a PBX level[9]. A diverse set of characterization techniques (microscopy, chemical analysis of purity, thermal properties, hazardous properties, HMX content, etc.) was applied to the as-received RDX crystal products. It appeared extremely difficult, however, to identify a specific property that would be able to serve as an indicator of the corresponding PBX quality, i.e. the shock sensitivity. In fact, it was difficult to obtain energetic crystals with one defect and to experimentally capture formation of hot spots at meso scales even with the advanced development of embedded gauges and other diagnostic techniques.

Recent dynamics molecular (MD) simulations with reactive force field (ReaxFF-MD) showed the potential for the technique to investigate formation of hot spots and propagation. Wood[10] used MD simulations to understand hot spot formation, characterization of the transition to deflagration and the importance of dynamical loading in their

DOI: 10.13009/EUCASS2019-368

criticality. They found that the collapse of a 40 nm diameter pore leads to a deflagration wave for shocks with particle velocities of 2 km/s. Shan[11] observed the transformation of an initial radially symmetric hot spot into a longitudinally asymmetric hot region extending over a much larger volume. Zhou[12] reported hot spot formation and chemical reaction initiation in shocked HMX crystal that was depended on the void size and impact strength. An[13] observed a hot spot forms at the nonuniform interface of RDX/HTPB, resulting in shear along the interface that leads to a large temperature increase. For energetic materials, this temperature increase may be coupled to chemical reactions that lead to detonation. It has been known that defects and heterogeneities concentrate shockwave energy in small regions, resulting in local excitation of the material. However, it still needs to make much effort to disclose shock-induced structural and chemical response of energetic materials by MD simulations, especially for energetic complex or PBXs.

The remained of this paper is organized as follows: section 2 describes the simulation and computational details, section 3 discusses the temperature and chemical response during the whole shock process. We also discussed structure damage and partial reactions at the initial stage and subsequent rapid decomposition of RDX and oxidation of active Al atoms. In section 4, we draw a conclusion about this work and provide some suggestions.

2. Simulation details

We used the ReaxFF reactive force field as implemented in a Large-scale Atomic Molecular Massively Parallel Simulator (LAMMPS) molecular dynamics package. ReaxFF is an advanced bond-order variable charge force field that enables large-scale simulations of chemically reactive systems. Full details of ReaxFF can be found elsewhere[14, 15]. The ReaxFF force field description for RDX/Al mixtures used in this paper[16] was developed for nitramines[17, 18] and was extended to the interaction between RDX and Aluminum (Al). We have shown that this force field accurately describes thermal decomposition and reasonably predicts shock properties of RDX/Al mixtures[19].

We used one-dimensional two-slab impact model to investigate the effect of single defect on dynamic deformation of RDX slab and chemical evolution of RDX/Al mixtures. Seven representative models constructed were shown in Table 1. One slab was composed of Al coated with a 3 nm thickness of alumina at both sides, which was short for "Aloxide60" hereafter. Active content of Al was set about 60%, just only to keep the weight ratio of RDX/Al similar to PBXN-109 (64wt%RDX/20wt%Al/HTPB). The other slab was the (210) oriented RDX crystal slab with single defect, including void, crack, dimple, angular edge, HMX molecules aligned with RDX crystal at different position. In model (b) of Table 1, a cylindrical void that contained only vacuum was 40 Å in diameter, while 16 Å gap within RDX crystal slab stood for a crack in model (c). In model (d), there was 3 nm deep hole on crystal plane (210) of RDX crystal. Wedge-shaped RDX crystal was cut down and the new crystal plane (100) was exposed in model (e). In model (f) and (g), HMX was added into RDX crystal by 5 wt%, which meant it contained 5760 numbers of RDX molecules and 216 HMX molecules in RDX/HMX/Aloxide60 or RDX/HMX/RDX/Aloxide60 sandwich models.

Table 1: Main information of the simulation models

Models	Defect type	Total atoms	Number of RDX molecules	Dimensions, Å	Density, g/cc
a	without defects	148768	5472	40.88×78.78×567.11	1.80
b	void	148936	5480	40.88×78.78×574.00	1.78
c	crack	148768	5472	40.88×78.78×573.48	1.78
d	dimple	148768	5472	40.88×78.78×572.89	1.78
e	angular	147088	5392	40.88×78.78×567.75	1.78
f	outer defects	160864	5760	40.88×78.78×609.94	1.78
g	inclusion of HMX	160864	5760	40.88×78.78×609.94	1.78

(a)RDX/Aloxide60;(b)RDXvoid40/Aloxide60;(c)RDXcrack16/Aloxide60;(d)RDXdimple/Aloxide60;(e)RDXangular/Aloxide60;(f)RDXouterHMX/Aloxide60;(g)RDXinnerHMX/Aloxide60

DOI: 10.13009/EUCASS2019-368

The two-slab impact model was first equilibrated at 5 K for 5 ps, then equilibrated at 300 K for 5 ps and annealed down to 5 K at a heating rate of 2K/ps. The optimized structures of those models are shown in Figure 1. The two slabs were set apart a certain distance to meet the actual density and to decrease non-bonded interaction at initial stage. After equilibration, all the atoms in the RDX slab were assigned an additional particle/impact velocity (Up) in the positive z direction and those in Al slab were assigned Up in the negative z direction. A three-dimensionally periodic boundary was imposed on these models to obtain chemical evolution of RDX/Al mixtures at a long simulation scale. The equations of motion of the atoms were integrated using the velocity Verlet discretization with a timestep of 0.1 fs. For full details of the molecular dynamics methodology, see Ref.[20].

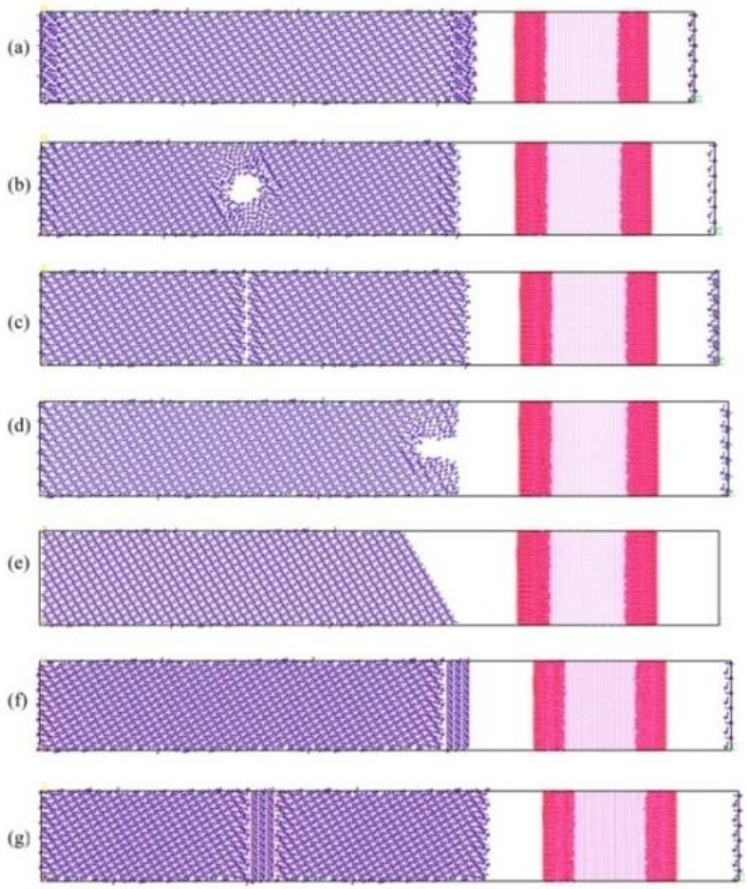

Figure 1: The optimized structures of RDX(210)/Al models with different defect. The symbol meaning of (a)~(g) is the same as that in Table 1.

3. Results and discussions

3.1 Analysis of the whole process

When the RDX crystal slab with single defect impacted against the Al slab in the opposite direction, a supported planar shockwave propagated through the RDX crystal from right to left along the [210] direction. Compressive stress wave made particle velocity diminish to zero rapidly and compressed each slab uniaxially. When compressive stress waves reached the free surface of the simulation cell, reflected tensile stress waves made stress decrease to zero and impelled particles move toward the periodic boundary. Then, another collision at periodic boundary generated. Subsequently, a series of compressive stress waves and tensile stress waves happened and the intensity gradually decreased. Although a better method may be used to suppress the reflected tensile stress waves into slab [21], this periodic boundary[20] could predict propagation of shock waves and accelerate chemical evolution of RDX/Al mixtures with the similar equilibrium products.

Figure 2 depicts temperature profile and the percentage of decomposed RDX molecules for seven kinds of RDX/Al models during the impact process at the initial particle velocity Up= 2.0 km/s. The main compressive stage after shockwave and secondary collision at the periodic boundary had been finished until at 30 ps. The percentage of

DOI: 10.13009/EUCASS2019-368

decomposed RDX molecules was about 20%. Then, the temperature rose rapidly, especially after 100 ps. At this stage, the temperatures in RDX/Al models with surface dimple or angular edge seemed to be faster than others. RDX/Al models with defects exhibited more active than RDX/Al model without defect, except RDX/Al models with outer HMX. The same conclusion was seen in the decomposition rate of RDX/Al models with different defect in Figure 2(b).

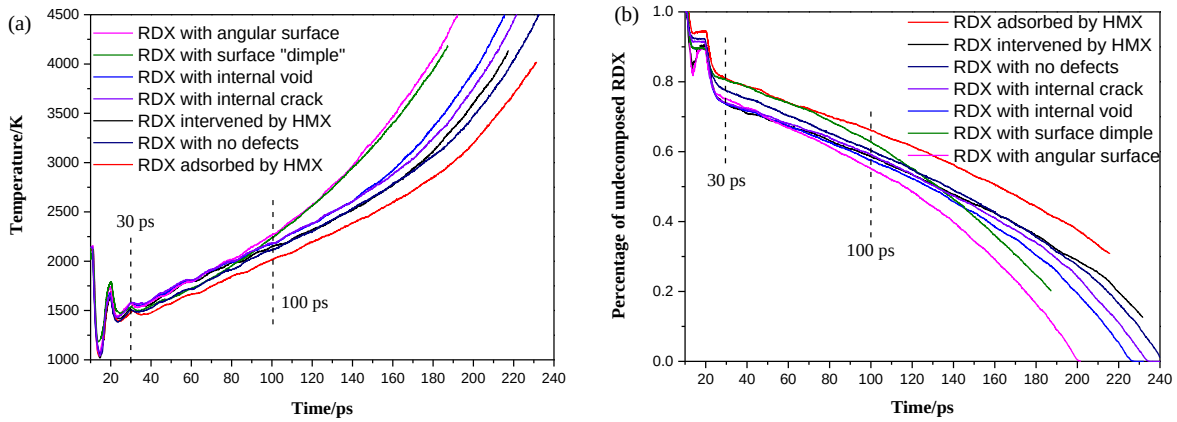

Figure 2: Temperature profiles (a) and the percentage of decomposed RDX molecules (b) for RDX/Al models with single defect during impact process with the initial particle velocity Up= 2.0 km/s.

3.2 Structure damage and partial reactions at the initial stage

Structure damage and partial decomposition were important for rapid decomposition of residue RDX molecules and for further oxidization of active Al atoms, so we further investigated the initial impact stage.
The loss weight percentage of RDX molecules in Figure 2(b) is statistically listed in Table 2.

Table 2: Statistical decomposed amount of RDX at different stages

models	Decomposed RDX, %		Rate constant at isochoric process, $\times 10^{-3}$ ps^{-1}
	Main impact	Second impact	
(a)RDX/Aloxide60	7.93	14.34	5.98
(b)RDXvoid40/Aloxide60	10.47	15.61	7.91
(c)RDXcrack16/Aloxide60	8.44	17.29	7.77
(d)RDXdimple/Aloxide60	10.48	8.64	8.12
(e)RDXangular/Aloxide60	11.12	10.38	8.14
(f)RDXouterHMX/Aloxide60	5.58	12.7	4.35
(g)RDXinnerHMX/Aloxide60	10.48	15.19	4.93

At shock-induced main compressive stage in Table 2, surface structure of RDX crystal slab with surface dimple or angular edge was severely damaged, which resulted in the most decomposed amount of RDX molecules in all RDX/Al models. The decomposed amount of RDX molecules with inner defects was also larger than that of RDX/Aloxide60. Inner HMX molecules played the same role in enhancing the initiation decomposition of RDX molecules with other defects, like void or outer dimple. However, the decomposition of RDX molecules was depressed at the presence of outer HMX molecules. At secondary collision stage at the periodic boundary, the decomposed amount of RDX molecules in RDX/Al models with void, crack or inner HMX was still larger than that in RDX/Aloxide60. The decomposed amount of RDX molecules with dimple, angular or outer HMX became fewer,

DOI: 10.13009/EUCASS2019-368

because there was not any defect lying at another side of each slab. From above, we see that RDX/Al models with inner defect can accelerate decomposition of RDX molecules at the whole shock stage. RDX/Al models with surface defect concentrate on the defect position to cause structure damage and local chemical reactions at initial compressive stage.

Figure 3 shows different population of decomposed RDX molecules at 30 ps. The middle slab in each snapshot was related to RDX slab with different defect, in which perfect RDX molecules were in green to make decomposed RDX molecules more discernible. The damaged RDX molecules concentrated at both sides of RDX slab and the secondary collision stage at the periodic boundary caused more numbers of RDX to decompose than the initial shockwave compressive stage. Taking RDX/Al model without any defects (model a) as a reference, there were a number of decomposed RDX molecules dispersed inside RDX slabs with void (model b), crack (model c) and inner HMX (model g) when compared with those in RDX slabs with surface defects (model d or e) and outer HMX (model f), indicating that internal defects played a key role in disordering crystal arrangement and in enhancing decomposition rate at initial impact stage.

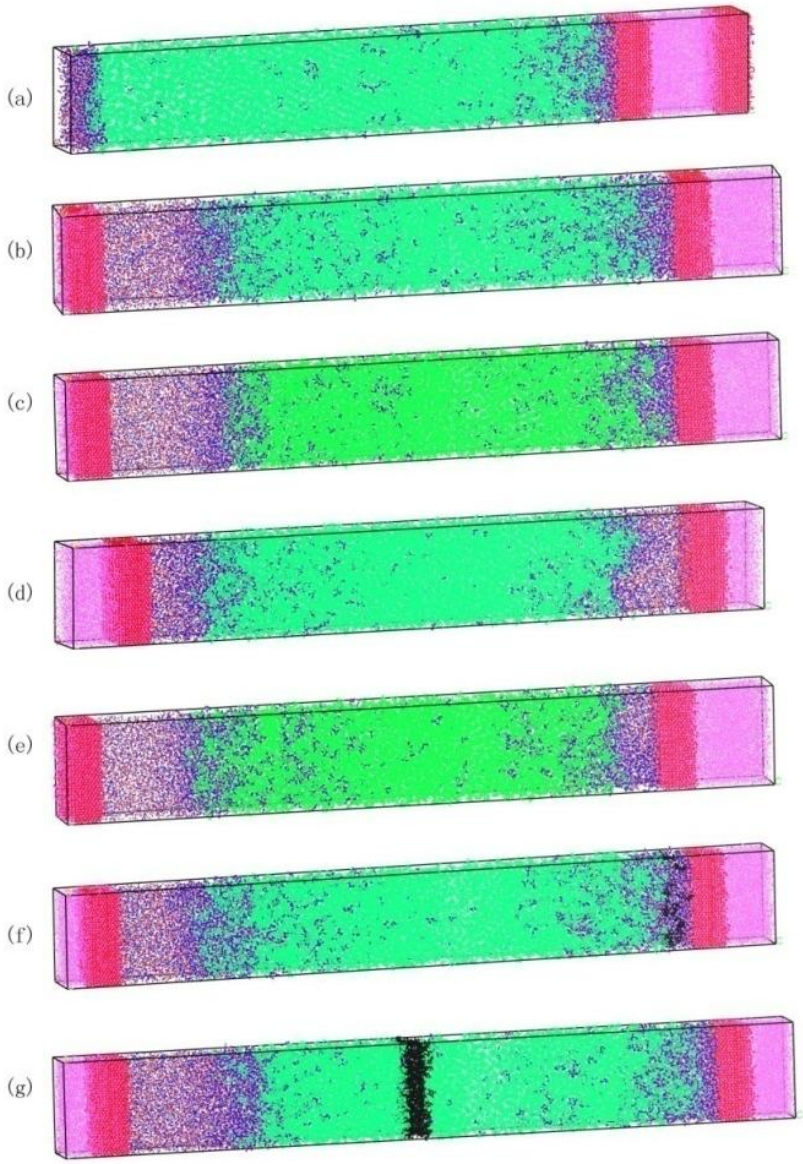

Figure 3: Snapshots of different RDX/Al model at 30 ps after shock loading. The perfect RDX molecules (green) and perfect HMX (black) illustrated no damage molecules. Other atom color scheme: Red, oxygen; magenta, aluminum; blue, nitrogen; green, carbon; white, hydrogen. The symbol meaning of (a)~(g) stands for (a) RDX/Aloxide60; (b)RDXvoid40/Aloxide60; (c)RDXgap16/Aloxide60; (d)RDXdimple/Aloxide60; (e) RDXangular/Aloxide60; (f) RDXouterHMX/Aloxide60; (g)RDXinnerHMX/Aloxide60.

DOI: 10.13009/EUCASS2019-368

3.3 Rapid decomposition of RDX and oxidation of active Al atoms

Table 2 also lists decomposition rate of RDX molecules after 30 ps at NVE (constant numbers, volume and total energy) ensemble condition. We found that one order exponential decay formula was good fit for decomposition rate of RDX molecules ($R^2 > 0.999$). The ranking of decomposition rates in RDX/Al models with different defect were RDXdimple/Aloxide60≈RDXangular/Aloxide60>RDXvoid40/Aloxide60≈RDXcrack16/Aloxide60>RDX/Aloxide60 >RDXouterHMX/Aloxide60≈RDXinnerHMX/Aloxide60. It was surprised that RDX decomposition rates in RDX/Al models with surface defects were faster than those in RDX/Al models with inner defects (void and crack) or inner HMX after 30 ps.

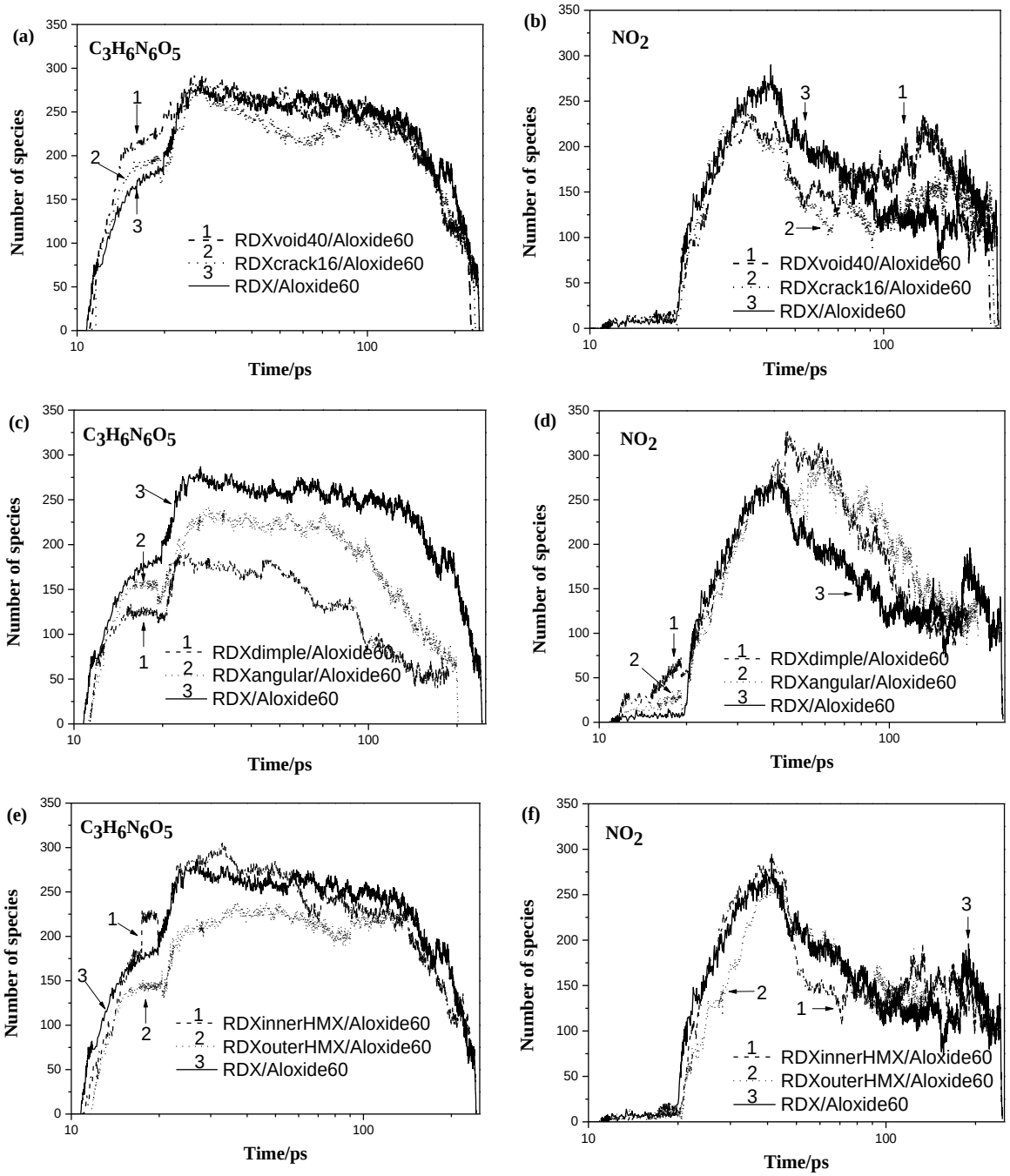

Figure 4: Time evolution of the concentration of initial main fragment $C_3H_6N_6O_5$ and active group NO_2 at Up= 2.0 km/s. For convenient comparison, the black line in each graph reflects changes in RDX/Al model without defect (RDX/Aloxide60).

DOI: 10.13009/EUCASS2019-368

In order to elucidate the discrepancy in chemical response between different RDX/Al models, we followed the tracks of initial fragments, active group, intermediate and final products. The evolution of initial main fragment $C_3H_6N_6O_5$ and active group NO_2 are presented in Figure 4.

A large number of fragment $C_3H_6N_6O_5$ existed due to the interaction between RDX molecule and alumina, which indicated the extent of chemical reaction at the interface. In Figure 4(a), the quantity of fragment $C_3H_6N_6O_5$ in RDX/Al models with void or crack at initial shock stage (< 25 ps) was more than that in RDX/Al models without defects and subsequently three kinds of models became almost the same. In Figure 4(c), the quantity of fragment $C_3H_6N_6O_5$ in RDX/Al models with dimple or angular edge was less than that in RDX/Al models without defects at the hole process. In Figure 4(e), the quantity of fragment $C_3H_6N_6O_5$ in RDX/Al models with inner HMX was very similar with that in RDX/Al models without defects, while the quantity of fragment $C_3H_6N_6O_5$ in RDX/Al models with outer HMX was lower. The difference in numbers of $C_3H_6N_6O_5$ indicated that the extent of chemical reaction at the interface was different in RDX/Al models, which was consistent with the initial structure damages. It was shown that main chemical reaction happened between RDX molecules and surface Al atoms at the interface for RDX/Al models with inner defects or inner HMX, while the predominant chemical reaction happened between RDX molecules for RDX/Al models with outer defects or outer HMX.

Active group NO_2, generated from homolytic fission of an N-N bond as the main initial dissociation path of RDX[22], can monitor decomposition process of RDX molecules. In Figure 4(d), the quantity of NO_2 in RDX/Al models with dimple or angular edge was more than that in RDX/Al models without defects within 25 ps. Subsequently, the maximum quantity of NO_2 was not only more than that of other RDX/Al models, but it lasted for a longer time, indicating that chemical reaction can be accelerated because of the large quantity of active species. This may be used to explain the rapid decomposition of RDX at later stage over 30 ps.

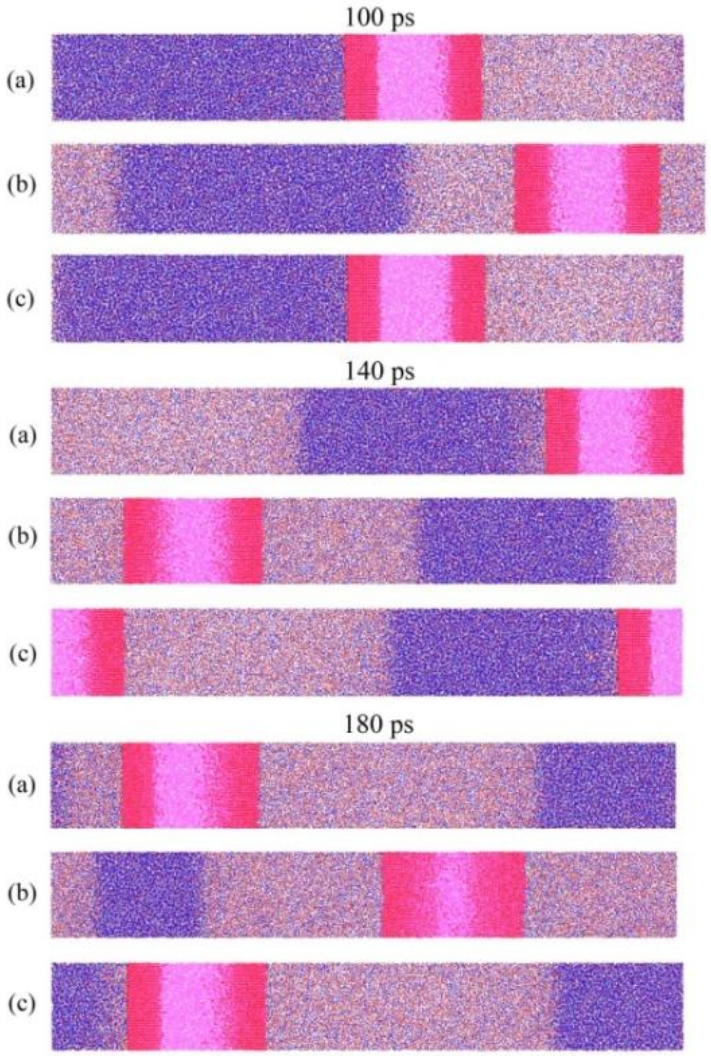

Figure 5: Snapshots for RDX/Al models with void(a), dimple(b) and without defect(c) at 100 ps, 140 ps and 180 ps, respectively. Color scheme: Red, oxygen; magenta, aluminum; blue, nitrogen; green, carbon; white, hydrogen.

DOI: 10.13009/EUCASS2019-368

We selected three RDX/Al models to further observe the location of chemical reaction at 100 ps, 140 ps and 180 ps, respectively, which was shown in Figure 5.

At 100 ps, the difference in temperature had become large and the chemical reactions located at the initial shock position obviously propagated in RDX/Al model with dimple. The reactions included initial decomposition of RDX molecules, secondary reaction of fragments and generation of final products, e.g. N_2, H_2O, CO_2 and HCN. The concentration of active group NO_2 was still high at 100 ps, which was seen in Figure 4(d). We believed that this led to the lasting chemical reaction at 140 ps and 180 ps. In comparison, the chemical reactions located at this position slowly propagated in RDX/Al model with void at 140 ps while it was seen at 180 ps for RDX/Al model without defect. Combined Figure 4 and Figure 5, it can be concluded that initial shockwave compression generated different structure damage and induced different chemical reaction paths due to the different RDX morphology and defect types.

In Figure 5, it also can be seen that oxidation of active Al atoms needed a long time although 45% of RDX molecules in number had been decomposed and high temperature reached over 2000 K in RDX/Al model with dimple at 100 ps. When simulation time arrived at 140 ps, partial active Al had been oxidized and the thickness of alumina layer coated on active Al continued to be increased. At 180 ps, only a few active Al atoms existed in RDX/Al model with dimple, but there were many active Al atoms still preparing for oxidation in the other two models. Quantity data that how many surplus active Al atoms exist at each simulation time are still being processed and does not present here.

3.4 The role of HMX molecules as defects in RDX crystals

According to military standards, type I RDX is allowed to contain up to 5% HMX and type Ⅱ RDX may contain 4-17% HMX. It was generally accepted that polymer bonded polymer that had low shock sensitivity contained RDX crystals with low HMX contents. We added extra 5 wt% HMX on RDX (210) crystal plane or put 5 wt% HMX between two parts of RDX, which can also be treated as sandwich structure. Figure 6 depicts the percentage of undecomposed RDX or HMX molecules for RDXouterHMX/Aloxide60 and RDXinnerHMX/Aloxide60 during the impact process at the initial particle velocity Up= 2.0 km/s. If HMX molecules were on RDX slab, HMX first met Al slab and composed over 60%, which resulted in few decomposition of RDX molecules. This was the reason why RDX decomposition rate was very slow in RDXouterHMX/Aloxide60. If HMX molecules lied between two parts of RDX, as outlined above in Figure 1(g), the role of inner HMX molecules was similar with void or crack, which accelerated decomposition of RDX molecules at the initial shock stage. It may explain that shock sensitivity of type Ⅱ RDX was high with the presence of a range of HMX content.

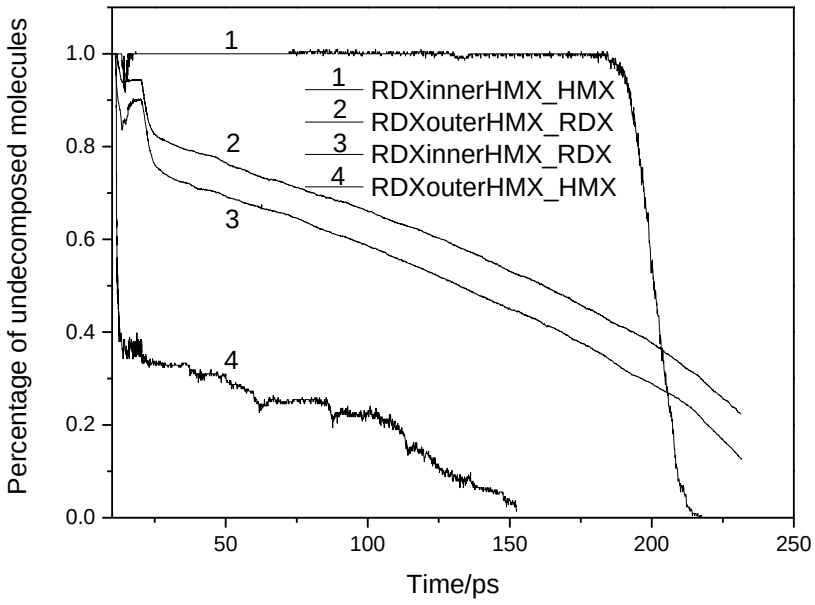

Figure 6: The percentage of undecomposed RDX or HMX molecules for RDX/Al models with outer HMX or inner HMX during impact process with the initial particle velocity Up= 2.0 km/s.

It was noted that RDX with low HMX did not mean it possessed low shock sensitivity, e.g. MI-RDX. Not only did the MI-RDX contained more surface defects, but also there were several different particle morphologies. It was this

DOI: 10.13009/EUCASS2019-368

difference in particle morphology and defect density that accounted for the differences in shock sensitivities between the I-RDX and MI-RDX.

4. Conclusions

We created RDX/Al models using two-slab impact model, one of which was composed of Al coated with a 3 nm thickness of alumina at both sides and the other one was RDX slab with single defect, including void, crack, dimple, angular edge, and extra HMX molecules on or between RDX crystal. We used a molecular dynamics simulation with ReaxFF force field to study single defect of RDX on shock sensitivity of RDX/Al mixtures. The results show that internal defects play a key role in disordering crystal arrangement and in enhancing decomposition rate at initial impact stage. RDX/Al models with surface defect concentrate on the defect position to cause structure damage and local chemical reactions to generate more active group NO_2, not interfacial reaction between RDX and Al slab. Minor content of HMX molecules exhibits different effects, which depends on the location whether on RDX surface or enclosed by RDX crystals. If HMX molecules are on RDX surface, the number of HMX molecules decompose over 60% before RDX and the presence of HMX result in slowing down decomposition rate of RDX/Al mixtures. If HMX molecules lie between two parts of RDX, the role of inner HMX molecules is similar with void or crack, which accelerate decomposition of RDX molecules at the initial shock stage. Initial products and quasi-equilibrium products were further discussed to analyze the different pathway of decomposition of RDX crystals with different defects.

It should be noted that there are still much work to study the effect of single defect of RDX crystals on shock sensitivity of RDX/Al mixtures. Further research could be focused on some important factors, e.g. model size effect, shock velocity and simulation time, void defect (size, shape and number), crack orientation, depth of surface defects, contents of HMX, other inclusions (solvent, water), et al.

References

[1] Bocksteiner, G., M. G. Wolfson, and D. J. Whelan. 1994. The critical diameter, detonation velocity and shock sensitivity of Australian PBXW-115. DSTO-TR-0076.

[2] Walley, S.M., J.E. Field and M.W. Greenaway. 2006. Crystal sensitivities of energetic materials. Mater. Sci. Technol., 22: 402-413.

[3] van der Heijden, A.E.D.M., R.H.B. Bouma and A.C. van der Steend. 2004. Physicochemical parameters of nitramines determining shock sensitivity. Propell. Explos. Pyrot., 29: 304-313.

[4] Borne, L. 1998. Explosive Crystal Microstructure and Shock Sensi-tivity of Cast Formulations. In: 11th Symposium (International) on Detonation. 657-663.

[5] Stoltz, C.A., B.P. Mason and J. Hooper. 2010. Neutron scattering study of internal void structure in RDX. J. Appl. Phys., 107: 103527.

[6] Hua, C., M. Huang, H. Huang, J.S. Li, F.D. Nie, and B. Dai. 2010. Intragranular Defects and Shock Sensitivity of RDX/HMX. Chin. J. Energ. Mater., 18: 152-157.

[7] Czerski, H. and W.G. Proud. 2007. Relationship between the morphology of granular cyclotrimethylene-trinitramine and its shock sensitivity. J. Appl. Phys., 102: 113515.

[8] Bellitto, V.J. and M.I. Melnik. 2010. Surface defects and their role in the shock sensitivity of cyclotrimethylene-trinitramine. Appl. Surf. Sci., 256: 3478-3481.

[9] Doherty, R.M. and D.S. Watt. 2008. Relationship between RDX properties and sensitivity. Propell. Explos. Pyrot., 33(1): 4-13.

[10] Wood, M.A., M.J. Cherukara, E.M. Kober, and A. Steinheil. 2015. Ultrafast Chemistry under Nonequilibrium Conditions and the Shock to Deflagration Transition at the Nanoscale. J. Phys. Chem. C, 119: 22008-22015.

[11] Shan, T.T., R.R. Wixom and A.P. Thompson. 2016. Extended asymmetric hot region formation due to shockwave interactions following void collapse in shocked high explosive. Phys. Rev. B, 94: 054308.

[12] Zhou, T.T., J.F. Lou, Y.G. Zhang, H.J. Song, and F.L. Huang. 2016. Hot spot formation and chemical reaction initiation in shocked HMX crystals with nanovoids: a large-scale reactive molecular dynamics study. Phys. Chem. Chem. Phys., 18: 17627.

[13] An, Q., S. V. Zybin, W. A. Goddard, Ⅲ, A. J. Botero, M. Blanco, and S. N. Luo. 2011. Elucidation of the dynamics for hot-spot initiation at nonuniform interfaces of highly shocked materials. Physical Review B, 84: 220101.

[14] Chenoweth, K., A. C. T. van Duin and W. A. Goddard, Ⅲ. 2008. ReaxFF Reactive Force Field for Molecular Dynamics Simulations of Hydrocarbon Oxidation. J. Phys. Chem. A, 112: 1040-1053.

[15] van Duin, A. C. T., S. Dasgupta, F. Lorant, and W. A. Goddard,Ⅲ. 2001. ReaxFF: a reactive force field for hydrocarbons. Journal of Physical Chemistry A, 105(41): 9396-9409.

DOI: 10.13009/EUCASS2019-368

[16] Wang, N., J.H. Peng, A.M. Pang, T.S. He, F. Du, and J.B. Andres. 2017. Thermodynamic simulation of the RDX-Aluminum interface using ReaxFF molecular dynamics. Journal of Physical Chemistry C, 121(27): 14597-14610.

[17] Strachan, A., E. M. Kober, A. C. T. van Duin, J. Oxgaard, and W. A. Goddard,Ⅲ. 2005. Thermal decompostion of RDX from reactive molecular dynamics. Journal of Chemical Physics, 122(5): 054502.

[18] Wood, M.A., A.C.T. van Duin and A. Strachan. 2014. Coupled thermal and electromagnetic induced decomposition in the molecular explosive αHMX; a reactive molecular dynamics study. Journal of Physical Chemistry A, 118: 885-895.

[19] Wang, N., J. Cheng, H.B. Li, F. Du, C.H. Li, J.J. Hu, and J.H. Peng. 2018. Dynamic evolution of aluminum particles subjected to RDX impact. Chem. Phys. Let., 695: 79-86.

[20] Wang, N., J.H. Peng, A.M. Pang, J.J. Hu, and T.S. He. 2016. Study on the anisotropic response of condensed-phase RDX under repeated stress wave loading via ReaxFF molecular dynamics simulation. Journal of Molecular Modeling, 22: 229.

[21] Cawkwell, M.J., T.D. Sewell, L.Q. Zhang, and D.L. Thompson. 2008. Shock-induced shear bands in an energetic molecular crystal: application of shock-front absorbing boundary conditions to molecular dynamics simulations. Physical Review B, 78: 014107.

[22] Schweigert, I.V. 2015. Ab initio molecular dynamics of high-temperature unimolecular dissociation of gas-phase RDX and its dissociation products. Journal of Physical Chemistry A, 119: 2747-2759.